Higher Order Structure of Chromatin: Evidence from Photochemically Detected Linear Dichroism†

Dipankar Sen, Sekhar Mitra, and Donald M. Crothers*
Department of Chemistry, Yale University, New Haven, Connecticut 06511
Received September 3, 1985; Revised Manuscript Received January 3, 1986

ABSTRACT: We have used photochemically detected linear dichroism to measure the separate average angular orientations of nucleosomes and linker DNA in 30-nm chromatin fibers of varying linker size (20–80 base pairs). Our results indicate that the average tilt angles vary with linker size, but not in a monotonic manner, suggesting that the constancy of geometry of the 30-nm fiber is maintained by compensatory changes of nucleosomal tilt which accommodate packing of variable lengths of linker DNA. We discuss the compatibility of our results with the various classes of models that have been proposed for the 30-nm fiber, including the continuous solenoid model and models built from the basic unit of the zig-zag ribbon. Many models can be eliminated, and all have to be modified to fit our results for chromatins with very long linkers.

DNA packaged as chromatin in eukaryotic nuclei may be regarded as consisting of two fundamental units: the chromatosome and linker DNA. The former contains a protein octamer made up of the core histones H2A, H2B, H3, and H4, around which is wrapped 166 base pairs (bp) of DNA in approximately two left-handed superhelical turns, with lysine-rich histone H1 or H5 positioned so as to clamp the ends of the 166 bp DNA segment (Simpson, 1978). The chromatosome is highly conserved as a structural unit over the entire range of eukaryotic chromatin. Linker DNA, however, varies greatly in length in chromatin from different sources, within different tissues from a single organism, and sometimes even within a single cell type (Thomas & Thompson, 1977). The length of DNA on a chromatosome, plus a single linker characteristic of the source of the chromatin, is defined as the "nucleosomal repeat" of that chromatin. In chromatins investigated to date, the repeat has been found to vary from 160 to 250 bp (Kornberg, 1977), implying linker lengths ranging from essentially 0 to about 80 bp.

At its lowest level of folding, observed in vitro at low ionic strength in the absence of multivalent cations, chromatin consists of a more or less extended chain of chromatosomes and linkers, the so-called "10-nm" fiber. Raising the monovalent ion concentration to 50 mM, or the divalent ion concentration to 250 μM, results in condensation of the 10-nm fiber into a "30-nm" fiber (Finch & Klug, 1976), which appears to correspond to the thick chromatin fiber seen in nuclei by electron microscopy (Olins & Olins, 1979). Electron microscopic observations of intermediates in the folding process have sometimes revealed a zig-zag chromatosome–linker DNA–chromatosome motif (Thoma et al., 1979; Worcel et al., 1981; Woodcock et al., 1984), but it remains uncertain whether this feature of the unfolded fiber is conserved in the 30-nm fiber (McGhee et al., 1983). Of particular interest is the observation (McGhee et al., 1983; Pearson et al., 1983; Allan et al., 1984) that all chromatins, regardless of linker size, form the typical 30-nm fiber under appropriate ionic conditions. How linkers of widely varying length can be packaged without substantially altering fiber geometry remains an unsolved problem.

The organization of the 30-nm fiber of chromatin of average nucleosomal repeat has been probed by a wide variety of techniques, including electron microscopy; X-ray, neutron, and light scattering; sedimentation; and electric and flow dichroism [reviewed by Butler (1983)]. The cumulative result of this work is a consensus view that the thick fiber probably consists of a somewhat irregular simple solenoidal helix of pitch about 11 nm, diameter 25–40 nm, and six to seven nucleosomes per helical turn. However, other structures have been proposed, including older models incorporating superbeads (Pruitt & Granger, 1980; Renz et al., 1977; Stratling et al., 1978, 1981; Zentgraf et al., 1980a,b) and newer proposals based on the further coiling of a flat zig-zag ribbon of nucleosomes (Worcel et al., 1981; Subirana et al., 1981; Woodcock et al., 1984).

Because of its sensitivity to DNA orientation, linear dichroism is capable of revealing details of the internal organization of the 30-nm fiber (McGhee et al., 1980, 1983; Lee et al., 1981; Lee & Crothers, 1982; Tjerneld et al., 1982; Yabuki et al., 1982; Allan et al., 1984). These studies have defined the limits of nucleosomal orientation within the fiber and, along with sedimentation measurements (Butler & Thomas, 1980; Thomas & Butler, 1980; Bates et al., 1981; Pearson et al., 1983; Butler, 1984), have contributed to the conclusion that the basic architecture of the fiber is surprisingly insensitive to linker size. Recently, photochemically detected linear dichroism has been used to determine separately the average dichroism of nucleosomal and linker DNA in calf thymus chromatin (Mitra et al., 1984), with the conclusion that the two kinds of DNA have different dichroism values and hence different orientations. This finding disfavors models in which nucleosomal DNA and linker DNA follow a continuous superhelical path; in addition, the strongly negative dichroism found for the linker in calf thymus chromatin rules out models such as the stacked nucleosomal ribbon diagrammed by Worcel et al. (1981), in which the linker DNA is arranged almost perpendicular to the fiber axis.

In this study, we use both optically and photochemically detected linear dichroism to probe the internal geometry of chromatins of varying linker length, using the photoreaction with psoralen to focus on the properties of the linker. The results show that the optical dichroism of chromatin fibers is nearly independent of linker length but that this constancy masks a substantial, mutually compensating, variation of linker and nucleosomal dichroism values. We conclude that both

† This work was supported by National Institutes of Health Grant GM 21966. S.M. was a fellow of the Jane Coffin Childs Memorial Fund.
* Correspondence should be addressed to this author.

0006-2960/86/0425-3441$01.50/0

nucleosomal and linker tilt angles are variables that can be adjusted to accommodate changes in the amount of linker DNA packaged in the fiber.

Photochemical Dichroism. The optical dichroism of the thick chromatin fiber is sensitive to the orientation of linker DNA and nucleosomal disks relative to the fiber axis, but since it is an average of the two contributions, one cannot deduce unambiguously the orientation of either of these structural elements from the optical measurement. Photochemically detected dichroism makes use of the property of the DNA binding family of drugs, the psoralens, to form covalent adducts preferentially with linker DNA when UV irradiated in the presence of chromatin fibers. Since the optical transition moment responsible for psoralen photoreaction is oriented roughly perpendicular to the DNA double-helix axis, the dichroism for the photoreaction yield can be used to determine the average DNA orientation (Mitra et al., 1984).

The experiment begins with dark equilibration of chromatin with ^{3}H-labeled (aminomethyl)trioxsalen (AMT), after which a brief electric field pulse ($\sim$15 kV/cm) is applied across the sample, and, with allowance for a delay time ($\sim$100 μs) to permit orientation, the solution is flashed with a polarized 308-nm pulse from an excimer laser. The extent of covalent attachment of AMT is assayed by scintillation counting of purified DNA extracted from the chromatin sample. Letting the photochemical yields for laser pulses polarized parallel and perpendicular to the electric field, normalized for variations in the laser pulse, be $Y_\parallel$ and $Y_\perp$, respectively, the photochemical dichroism (ρ_{pc}) at field E is computed from the ratios $R_\parallel = Y_\parallel(E)/Y_\parallel(E=0)$ and $R_\perp = Y_\perp(E)/Y_\perp(E=0)$ according to

$$\rho_{pc} = \frac{3(R_\parallel - R_\perp)}{2R_\perp + R_\parallel} \quad (1)$$

Materials and Methods

Chromatin was prepared from HeLa cells, prepelleted and frozen chicken erythrocytes, and freshly extracted sperm from the sea urchin *Strongylocentrotus purpuratus* (sea urchins from Alacrity Marine, Rodondo Beach, CA) essentially as described by McGhee et al. (1983), with the following modifications: purified sea urchin sperm nuclei were digested for only 6–7 h at 37 °C with *Hae*III at 200 units/mL, and the digestion mixture was diluted 2–3-fold with 1 mM tris(hydroxymethyl)aminomethane (Tris)/0.25 mM ethylenediaminetetraacetic acid (EDTA), pH 7.5, prior to overnight dialysis with two changes against this same buffer. Substantial solubilization of higher molecular weight chromatin fragments was achieved in this way. The central portion of the sucrose gradient profile was collected and used for dichroism experiments; the DNA size was 12 ± 4 kilobases (kb). No sliding of nucleosomes is expected under the low-salt isolation conditions employed nor was there any evidence for that phenomenon in gel electrophoretic analysis of the DNA products of micrococcal nuclease digestion of chromatin samples.

Dichroism experiments were carried out in 0.2 mM Tris, 0.3 mM NaCl, and 0.003 mM EDTA, pH 7.5, with $MgCl_2$ added as indicated, as well as in the buffer 0.13 mM cacodylic acid, 0.12 mM NaOH, and 0.003 mM Na_2EDTA, pH 7, used by McGhee et al. (1983). The results of dichroism experiments performed in the two buffers were essentially indistinguishable.

The procedures of the photochemical dichroism experiment and the various control experiments to determine the linearity of light dose–response for chromatin–AMT covalent bond formation are described in detail by Mitra et al. (1984). During the repeated ethanol precipitations of deproteinized chromatin samples from the photochemical dichroism experiments, sodium dodecyl sulfate (SDS) was added to 0.1% for the first two ethanol precipitations. The detergent helped to sequester noncovalently bound AMT, reducing the background ^{3}H counts to extremely low levels, and yielded a signal to noise of typically 10 to 1. Three pulses of the excimer laser per sample were usually required to obtain a satisfactory level of AMT attachment to chromatin DNA. At the levels of added AMT used, approximately 1 per 200 bp, our earlier experiments (Mitra et al., 1984) demonstrated that there is no detectable distortion of the chromatin fiber, as judged by the criterion of optical dichroism.

Quantitation of relative AMT binding to nucleosomal and linker regions of HeLa and sea urchin sperm chromatin was carried out as described by Mitra et al. (1984). In both cases, relative AMT binding to monomers as compared to dimers was measured to determine relative binding to linkers and nucleosomes.

Results

Magnesium Concentration Dependence of Chromatin Optical Dichroism. Accurate and meaningful results from photochemical dichroism experiments require that experiments be performed (a) at a concentration of Mg^{2+} which assures optimal compaction without substantial aggregation of the fibers and (b) at an electric field high enough to bring the fiber to full orientation in the field, but not of sufficient strength to produce structural distortion. In a recent study (Sen & Crothers, 1986), we described the influence of multivalent cations on chromatin condensation, concluding that 250 μM Mg^{2+} produces the maximum rotational relaxation rate and hence the optimal compaction required by criterion a; higher Mg^{2+} concentrations yield progressive aggregation.

Concerning criterion b, Figure 1 shows that the electric field dependence of the dichroism amplitude of chicken erythrocyte and sea urchin sperm chromatin is strongly dependent on Mg^{2+} concentration; the data for HeLa cell chromatin (not shown) were very similar to those determined for chicken erythrocyte samples. In all three cases, at chromatin concentrations of 30 μM DNA–phosphate, one observes a plateau in the field dependence of ρ at fields above 15 kV/cm, but only if the Mg^{2+} concentration equals or exceeds 250 μM. This, as we showed earlier for chromatin fibers stabilized by cross-linking (Lee et al., 1982), is the behavior expected for particles which orient by an induced dipole moment mechanism and can only mean that full orientation has been achieved by $E \geq 15$ kV/cm when the Mg^{2+} concentration level equals or exceeds that required ($\sim$250 μM) for optimal compaction.

In contrast, McGhee et al. (1983) state that they observe full compaction of the chromatin, and a corresponding leveling off of limiting dichroism values (extrapolated to infinite field), when there are one to two Mg^{2+} ions present per chromatin phosphate, corresponding to less than 100 μM Mg^{2+}. Comparison of their dichroism amplitudes with ours indicates that they may have assumed a premature plateau in the dependence of dichroism amplitude on Mg^{2+} concentration. Thus, for sea urchin sperm chromatin, they measured a (extrapolated) limiting dichroism of −0.26, approximately twice the value we obtain directly from the plateau in Figure 1. The difference is due to the increase of ρ with E observed at suboptimal concentrations of Mg^{2+}, as seen in Figure 1, a phenomenon we believe to be due to electric field induced distortion of chromatin fibers containing insufficient Mg^{2+}. A likely source of this effect is the substantial permanent dipole moment of the nucleosome (Crothers et al., 1978), resulting in its local orientation at high fields unless sufficient Mg^{2+} is added to

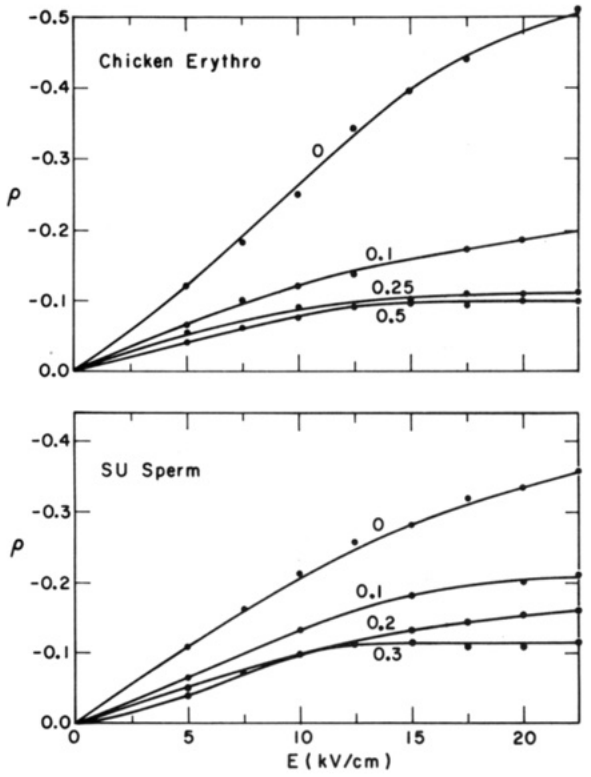

FIGURE 1: Electric field dependence of the optical dichroism amplitude at different Mg^{2+} concentrations. The dichroism amplitude ($-\rho$) for chicken erythrocyte (upper panel) and sea urchin sperm (lower panel) chromatins is shown as a function of electric field strength (E) for different concentrations of added $MgCl_2$, expressed in millimolar units adjacent to each curve.

Table I: AMT Distribution in Monomer and Dimer Nucleosomes[a]

particle	^3H cpm	DNA amount	cpm/bp	DNA size
monomer (HeLa)	2455	20.4	120	160 ± 15
dimer (HeLa)	2837	16.4	173	343 ± 25
monomer (SU sperm)	4120	30.0	137	160 ± 15
dimer (SU sperm)	3789	15.4	246	400 ± 30

[a] DNA or base pair amounts are in arbitrary units. DNA sizes are given in base pairs.

stabilize the fiber against distortion by the field.

In a recent electric dichroism study, Allan et al. (1984) found that full compaction of zero-linker chromatin from bovine cortical neurons is attained only at a Mg^{2+} to DNA–phosphate level of 8 to 1, consistent with our results. Also, their reported limiting dichroism of −0.1 for zero-linker chromatin is in agreement with our observation that the limiting dichroism of all optimally compacted, Mg^{2+}-containing chromatins, regardless of linker size, lies within ±0.03 of −0.1.

Previous publications from our laboratory (Lee & Crothers, 1982; Yabuki et al., 1982) reported the appearance of a field-dependent nondichroism signal, reflecting a field-induced absorbance decrease of the chromatin sample. In our recent experiments, we have found that this signal is the consequence of the repeated high-field pulses to which the sample was exposed, at least for non-cross-linked material. Pulsing

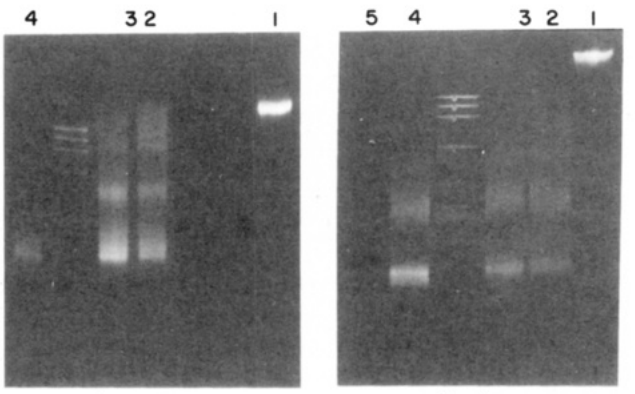

FIGURE 2: Micrococcal nuclease digestion products from [^3H]-AMT–chromatin complexes. Deproteinized, ethanol-precipitated DNA samples from sea urchin sperm (left) and HeLa cell (right) chromatin were run on a 1% agarose gel. In each gel, lane 1 represents an undigested control; lanes 2, 3, 4, and 5 are the digestion products after 0.5, 1, 5, and 10 min, respectively, of digestion with 30 units/mL staphylococcal nuclease at 37 °C, with a chromatin concentration of approximately $A_{260} = 0.3$.

chromatin samples no more than twice at fields of 20 kV/cm or higher eliminated the problem.

Photochemical Dichroism Experiments. The results of experiments to determine the relative distribution of photoreacted AMT molecules in linker and chromatosomal DNA from HeLa and sea urchin sperm are shown in Figure 2 and Table I. From the ratio of [^3H]AMT counts to the ethidium fluorescence intensity of each gel band, the ratio of bound AMT per DNA base pair was determined for monomer (chromatosomal) and dimer DNA. Taking the dimer to consist of two chromatosomes plus one linker, we calculated the fraction of bound AMT which is attached to the linker, finding 48% ± 10% for HeLa and 72% ± 8% for sea urchin sperm.

The results of the photochemical dichroism experiments for the two chromatins are shown in Table II. From the data presented, we were able to calculate the separate dichroism values for linker and nucleosomal disks, with the results collected in Table III.

Orientation of Nucleosomal Disks and Linker DNA. We assume that the 166 bp chromatosomal DNA can be approximated for dichroism purposes by two superhelical turns, with a small ratio of pitch to diameter. With these assumptions, the particle dichroism is given by (Crothers et al., 1978)

$$\rho_n = (3/8)(3\cos^2\gamma_n - 1) \quad (2)$$

where γ_n is the angle formed between the fiber axis and the normal to the plane of the nucleosomal disk.

In the absence of rigorous geometric information about the conformation of various linkers, we may consider two limiting cases for their shape, namely, an integral multiple of half-superhelical turns, for which the linker dichroism ρ_l is analogous to that given above for the nucleosomal disk, or a rigid rod, for which the dichroism is

$$\rho_l = -(3/4)(3\cos^2\beta - 1) \quad (3)$$

where β is the angle between the linker DNA rod and the fiber

Table II: Photochemical and Optical Dichroism

species	linker (bp)	linker AMT distribution (%) nucleosome	linker	ρ_{pc}	$\rho_{optical}$
HeLa	20	52 ± 10	48 ± 10	+0.01 ± 0.06	−0.11 ± 0.01
calf thymus	34	40 ± 10	60 ± 10	−0.23 ± 0.04	−0.09 ± 0.01
SU sperm	77	28 ± 2	72 ± 8	+0.12 ± 0.03	−0.13 ± 0.01

Table III: Dichroism and Orientation Angles for Nucleosome and Linker DNA[a]

species	linker (bp)	ρ_nndγ_n (deg)	γ_n (deg)	ρ_l	γ_l (deg)	β_l (deg)
ox cort[c]	0	−0.10	60 ± 3			
HeLa	20	−0.16	64 ± 3	+0.20	44	60
calf thymus[b]	34	−0.04	57 ± 3	−0.36	83	45
SU sperm	77	−0.32	77 ± 3	+0.29	40	61

[a] The angle γ, calculated from eq 2, is that between the fiber axis and the normal to the nucleosomal disk, or the normal to a plane containing a linker considered to contain an integral number of semicircular turns. The angle β is measured between the fiber axis and the DNA double-helix axis for a linker considered to be a straight rod. The subscripts n and l refer to nucleosome and linker, respectively. [b] From Mitra et al. (1984). [c] From Allan et al. (1984).

axis. An important assumption underlying this analysis is that the AMT molecules are randomly bound to the linker, so that they reflect the average DNA dichroism in the linker (Mitra et al., 1984). This assumption is supported by our observation that the photochemical dichroism does not change when the psoralen to chromatin base pair ratio is varied from 1:200 to 1:25.

Discussion

General Implications. From the results collected in Tables II and III, we are able to draw some general conclusions about fiber structure which do not require that we assume a specific model. We note first the striking uniformity of the optical dichroism of the fiber, nearly independent of linker size between 0 and 80 bp. However, upon separating the dichroism into its nucleosomal and linker components, it is found that the nucleosomal contribution does vary, ranging from −0.04 for calf thymus to −0.32 for sea urchin sperm chromatin. These values imply that the tilt of the nucleosomal disks relative to the fiber axis (the tilt angle is $90° - \gamma_n$) varies from 33° to 13°. Hence, average nucleosomal tilt is a reasonably flexible entity in fiber construction, and the observed range is presumably that required to accommodate the range of linker sizes found in nature. An extreme, presumably nonphysiological, value of 39° for the tilt was estimated for dimethyl suberimidate cross-linked calf thymus chromatin (Lee et al., 1981); this angle may represent an upper limit to the internal tilt flexibility in chromatin of 200 bp repeat length.

As a further general observation, we note that the average nucleosomal dichroism neither changes in a monotonic and predictable manner, as inferred by McGhee et al. (1983), nor is constant for all chromatins, as proposed by Butler (1984). A corresponding nonmonotonic variation of linker dichroism is also seen, with a rather large negative dichroism for the midsized calf thymus linker and positive values for the shorter (HeLa) and longer (sea urchin) linkers. (Note that the more negative the dichroism, the greater the projection of the linker DNA axis along the fiber axis, whereas positive dichroism values imply that the linker DNA has a greater projection perpendicular to the fiber axis than parallel to it.) Therefore, short and long linker DNAs have a predominant projection perpendicular to the fiber axis, but this is not the case for the mid-sized calf thymus linkers, whose parallel and perpendicular projections are nearly equal.

Orientation of the Nucleosome Dyad Axis. Our experiments set values for the tilt angle of nucleosomes relative to the fiber axis, but full knowledge of nucleosome orientation requires that we establish the value of another variable, specifically the angular orientation of the nucleosome dyad axis. Our present results provide suggestive, but not definitive, indications on that subject.

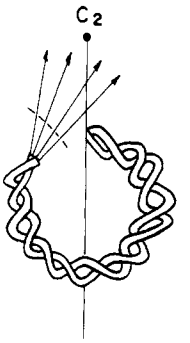

FIGURE 3: DNA exit angle from the nucleosome. Half of the (approximately) 2-fold symmetric DNA of a core particle is shown, adapted from Richmond et al. (1984). The DNA backbone drawn is half of 135 bp long; the dashed line indicates the probable position of the end of the DNA of a 146 bp nucleosomal core particle. The arrows indicate possible directions that might be adopted by the DNA helix axis as it exits the core particle. The results of earlier dichroism studies (Crothers et al., 1978; Mandelkern, 1980) suggest that the exit vector is more parallel than perpendicular to the dyad or C_2 axis of the particle.

Earlier experiments on the dichroism of larger (~175 bp) nucleosomes (Crothers et al., 1978) and H1-containing chromatosomes (Mandelkern, 1980) showed a more negative dichroism for these larger particles than for 146 bp DNA-containing core particles. This result implies that the additional DNA added onto the core particle structure (Figure 3) must exit the nucleosome with substantial projection along the electric field orientation direction, which is equivalent to the dyad or C_2 axis. This interpretation is consistent with recent structural work (Richmond et al., 1984) which indicates that protruding histone H2A molecules near the DNA entry and exit points prevent that chain from continuing on a circular path, which would yield a predominant DNA projection perpendicular to the nucleosome dyad.

Unless there is a sharp DNA bend just at the point where it merges into the linker, one expects the first part of the linker DNA to continue on the path established by its nucleosome exit angle, with projection primarily along the particle dyad axis. Therefore, it is plausible to equate the orientation of a short linker with the orientation of the nucleosome dyad axis. Since the dichroism of the linker is positive in short-linker chromatin, we consider it likely that the nucleosome dyad axes are predominantly perpendicular to the fiber axis. Clearly, this tentative conclusion needs to be verified by a direct experiment.

Comparison with Existing Models. Among the various structures proposed for the 30-nm fiber in the form of a solenoid, the most detailed is the "superhelical spacer" model described by McGhee et al. (1983). According to this proposal, the linker DNA continues on a superhelical path whose axis is defined by the curve through the chromatosome centers and whose diameter is that of the chromatosome, or 11 nm. Variable linker length is accommodated by varying the pitch of the DNA superhelix in the linker ("spacer") region. The model predicts that linker dichroism should become more negative as linker length increases; for sea urchin sperm chromatin, the linker dichroism should be nearly the same as the nucleosomal dichroism. These predictions clearly contradict our results. Indeed, we do not see how any general model in which the linker and nucleosomal DNAs follow a continuous superhelical path can be accommodated to the substantial positive linker dichroism we find for sea urchin sperm chromatin, in which the 80 bp linker would contribute a full superhelical turn, with a conformation necessarily very similar to that of nucleosomal DNA.

The twisted helical ribbon model of Worcel et al. (1981) and the helical ribbon model of Woodcock et al. (1984) are prototypical of those based on a zig-zag chromatosome–linker–chromatosome–linker motif as the fundamental unit for higher order packing. In these models, nucleosome dyad axes alternate in pointing roughly up and down along the 30-nm fiber axis, with even- and odd-numbered nucleosomes forming separate layers in the solenoidal helix. The layers are connected by linker DNA, which must consequently be oriented predominantly parallel to the fiber axis, yielding negative linker dichroism, and increasingly so as linker length is increased. Again, this feature is contrary to our results. In addition (although this objection is not directly related to our dichroism results), it is difficult to accommodate 80 bp linear linkers in such structures, since this would require that the edges of successive nucleosome layers be half the linker length, or over 10 nm apart.

The reverse loop and bulge loop models described by Butler (1984) address directly the problem of packaging linkers of varying sizes and seek to accommodate the geometrical features to the available electric dichroism data. In the proposed structures, linkers occupy the central core of the solenoidal helix, either adopting a right-handed superhelical conformation, which is opposite in handedness to the nucleosome DNA superhelix (reverse loop model), or forming a bulge in the solenoid core, thus adding half a left-handed superhelical turn to the 1.5 turns contributed by the nucleosome. Dichroism values for linker and nucleosome were calculated on the basis of an assumption which is inconsistent with our results, namely, that nucleosome tilt is independent of linker length. (The main basis for the assumption was the observed equality of sedimentation coefficient for chromatin fibers containing equal numbers of nucleosomes but different linker lengths; this comparison neglects the sedimentation coefficient increase expected on the basis of the increased mass contributed by the linker. Furthermore, it is doubtful that sedimentation coefficient measurements have sufficient sensitivity to detect the small changes in fiber dimensions that might accompany alterations in the angular orientation of the nucleosomes.)

The linker dichroism values calculated by Butler (1984) for linkers corresponding to HeLa, calf thymus, and sea urchin chromatin, respectively, are −0.38, −0.56, and −0.69 (reverse loop model) and +0.30, +0.39, and +0.57 (bulge loop model); the corresponding values from our experiments are +0.20, −0.36, and +0.29. It seems that neither model as proposed predicts the trends adequately.

Besides differing in calculated linker dichroism values, Butler's two models also make different predictions about the change in linking number when DNA is packaged into chromatin. The right-handed linker superhelix in the reverse loop model compensates one of the approximately two writhe turns on the nucleosome, giving a writhe increment per nucleosomal repeat unit of $\Delta Wr \approx -1$, whereas in the bulge loop model, $\Delta Wr \approx -2$. Assuming the conclusion of Klug and Lutter (1981) to be correct, the helical screw of DNA on the nucleosome changes from 10.5 to about 10.0 bp per turn, producing a twist increment per nucleosome of $\Delta Tw \approx +1$. The net of these is a predicted linking number increment of $\Delta Lk \approx 0$ for the reverse loop model, and $\Delta Lk \approx -1$ for the bulge loop model; these values should be compared with the experimental estimates of $\Delta Lk \approx -1$ to −2 (Germond et al., 1978; Stein, 1980).

Modified Models. In our view, at least two basic classes of models remain viable at this time, considering the limited structural information available about the internal organization of the 30-nm fiber. These include the basic solenoidal helix with linkers internal to the solenoid and helical ribbon models based on the zig-zag chain. Both, however, require alteration of their previously proposed forms in order to be consistent with our results.

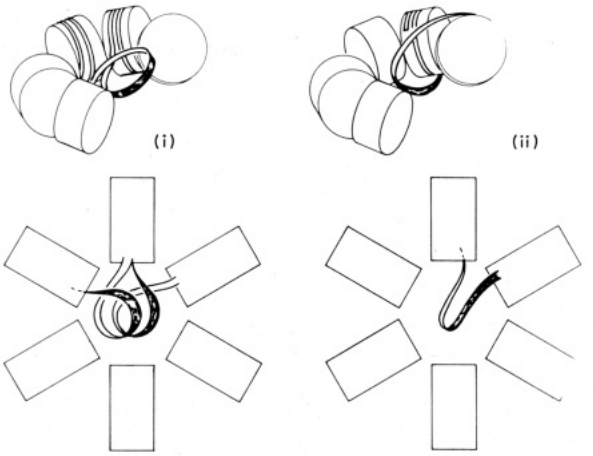

FIGURE 4: Reverse and bulge loop models modified to yield positive dichroism for long-linker chromatin. Conformation i is the reverse loop model shown in a cut-away, transverse view (upper) and an end-on view (lower). Conformation ii is the bulge loop model shown in similar views. The increased tilt of the linker loop produces the observed positive dichroism; this geometry may facilitate packing the linker DNA in the central solenoidal cavity.

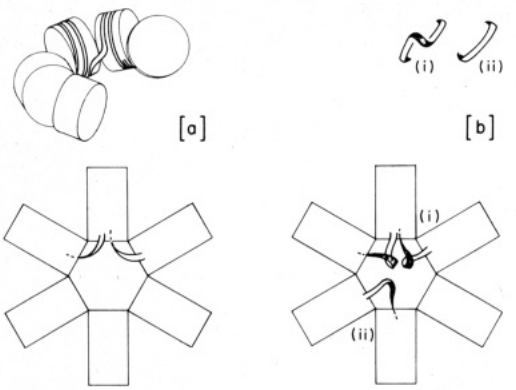

FIGURE 5: Solenoid with internal linkers for short and medium length linkers. As shown in (a), the linker for HeLa cell chromatin can pass in a small loop from one nucleosome to the next, with a sufficient tilt to yield positive dichroism. Intermediate-sized linkers, such as found in calf thymus chromatin, are shown in (b), with models falling in the reverse loop and bulge loop classes indicated in conformations i and ii, respectively. Negative dichroism for these linkers probably requires relatively sharp DNA kinks.

Figures 4 and 5 depict possible variations of linker conformation in the internal linker model. As shown in Figure 4, it is relatively easy to devise structures which fit the positive dichroism observed for long-linker (~80 bp) chromatin: one need simply tilt the reverse loop postulated by Butler (1984) (Figure 4, conformation i) or appropriately flatten the path of the bulge loop (Figure 4, conformation ii). There seems to be no reason in principle why the writhe increment per nucleosome need be an integer for such models, nor need it be independent of linker length. The fit to a positive dichroism for short-linker chromatin is also unproblematic, as illustrated in Figure 5a for chromatin containing approximately 20 bp of linker.

We found it not quite so easy to model linker conformations which would naturally lead to negative dichroism values for mid-sized linkers such as in calf thymus chromatin. Two schematic drawings are shown in Figure 5b, where confor-

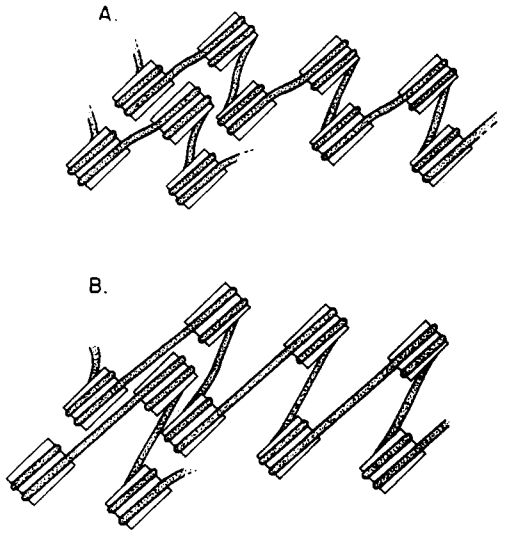

FIGURE 6: Possible modification of the helically wound zig-zag ribbon model. This model differs from previous proposals (Worcel et al., 1981; Subirana et al., 1983; Woodcock et al., 1984) in that nucleosomes in one layer of the helix are separated by an intercalated nucleosome from the layer below. The view shown here is normal to the surface of the solenoid at all points, with the solenoidal axis lying vertically in the page. (A) and (B) differ in linker length; increased linker length is compensated by sliding the intercalated nucleosome relative to its neighbors in the layer. An advantage to models of this kind is that the dipole moments of nucleosomes stacked face to face in a layer alternate in direction, an energetically favorable conformation; in addition, nucleosomes which interact edge to edge do so with their dipole moments aligned parallel, again a favorable configuration.

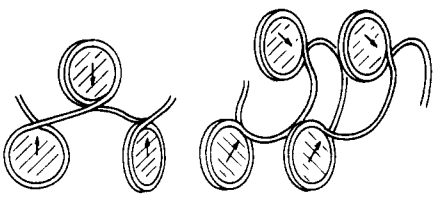

FIGURE 7: Schematic model showing arcing of long linkers in the helical zig-zag ribbon toward the central cavity of the solenoid. In this model, designed to help accommodate long linkers (B) compared to short linkers (A), the nucleosome dyad axes (arrows) are neither parallel nor perpendicular to the solenoid axis but alternate up and down in direction, thus preserving the nonpolar character of the fiber.

mation i is related to the reverse loop class and conformation ii is essentially a bulge loop. Building either of these models with a linker conformation having sufficiently negative dichroism seems to require rather sharp DNA kinks.

Figure 6 illustrates a modification of the helical zig-zag chain model which makes it easier to accommodate linkers of varying size, showing "intercalation" of odd-numbered nucleosomes from the preceding turn of the helix between adjacent even-numbered nucleosomes. An additional advantage of such models is that one predicts favorable interaction energies between the nucleosome dipole moments, which point in opposite directions along the linker axis for odd- and even-numbered nucleosomes in Figure 6. The problem of the linking number in helical zig-zag chain models is discussed by Worcel et al. (1981).

Our dichroism results require modification of the linker conformation from the stylized pattern shown in Figure 6, or from the simple connecting conformation in the more standard helical zig-zag ribbon, because of the nonmonotonic variation of linker dichroism with length. One possibility is shown in Figure 7, in which the 80 bp linkers form arcs which bend into the central cavity of the solenoidal helix. A favorable consequence for long linkers is a shortening of the distance, measured along the fiber axis, separating adjacent nucleosomes in the zig-zag chain.

Final solution of the structure of the 30-nm chromatin fiber will probably require integration of information from a variety of sources. Until such crucial variables as the orientation of the nucleosome dyad axes, the helical twist of DNA on the nucleosome, and the possible dependence of linking number increment on chromatin repeat length are firmly agreed upon, it seems advisable to keep the basic options open.

ACKNOWLEDGMENTS

We thank Marilyn Newman for gifts of HeLa cells, Dr. Steven Colson for advice on the laser experiments, and Suzan Vrba for secretarial assistance.

REFERENCES

Allan, J., Hartman, P. G., Crane-Robinson, C., & Aviles, F. X. (1980) *Nature (London) 288*, 675–679.
Allan, J., Rau, D. C., Harborne, N., & Gould, H. (1984) *J. Cell Biol. 98*, 1320–1327.
Butler, P. J. G. (1983) *CRC Crit. Rev. Biochem. 15*, 57–91.
Butler, P. J. G. (1984) *EMBO J. 3*, 2599–2604.
Crothers, D. M., Dattagupta, N., Hogan, M., Klevan, L., & Lee, K. S. (1978) *Biochemistry 17*, 4525–4533.
Finch, J. T., & Klug, A. (1976) *Proc. Natl. Acad. Sci. U.S.A. 73*, 1897–1901.
Germond, J.-E., Hirt, B., Oudet, P., Gross-Bellard, M., & Chambon, P. (1975) *Proc. Natl. Acad. Sci. U.S.A. 72*, 1843–1847.
Keller, W., Muller, U., Eickel, I., & Zentgraf, H. (1978) *Cold Spring Harbor Symp. Quant. Biol. 42*, 227–244.
Klug, A., & Lutter, L. C. (1981) *Nucleic Acids Res. 9*, 4267–4283.
Kornberg, R. D. (1977) *Annu. Rev. Biochem. 46*, 931–934.
Langmore, J. P., & Schutt, C. (1980) *Nature (London) 288*, 620–622.
Lee, K. S., & Crothers, D. M. (1982) *Biopolymers 21*, 101–116.
Lee, K. S., Mandelkern, M., & Crothers, D. M. (1981) *Biochemistry 20*, 1438–1445.
Mandelkern, M. (1980) Ph.D. Thesis, Yale University.
McGhee, J. D., Rau, D. C., Charney, E., & Felsenfeld, G. (1980) *Cell (Cambridge, Mass.) 22*, 87–96.
McGhee, J. D., Nickol, J. M., Felsenfeld, G., & Rau, D. C. (1983) *Cell (Cambridge, Mass.) 33*, 831–841.
Mitra, S., Sen, D., & Crothers, D. M. (1984) *Nature (London) 308*, 247–250.
Olins, A. L., & Olins, D. E. (1977) *Science (Washington, D.C.) 183*, 330–332.
Pearson, E. C., Butler, P. J. G., & Thomas, J. O. (1983) *EMBO J. 2*, 1367–1372.
Pruitt, S. C., & Grainger, R. M. (1980) *Chromosoma 78*, 257–274.
Renz, M., Nehls, P., & Hozier, J. (1977) *Proc. Natl. Acad. Sci. U.S.A. 74*, 1879–1883.
Richmond, T. J., Finch, J. T., Rushton, B., Rhodes, D., & Klug, A. (1984) *Nature (London) 311*, 532–537.
Sen, D., & Crothers, D. M. (1986) *Biochemistry 25*, 1495–1509.
Stein, A. (1980) *Nucleic Acids Res. 8*, 4803–4820.
Stratling, W. H., & Klingholz, R. (1981) *Biochemistry 20*, 1386–1392.
Stratling, W. H., Muller, U., & Zentgraf, H. (1978) *Exp. Cell Res. 117*, 301–311.

Subirana, J. A., Munoz-Guerra, S., Radermacher, M., & Frank, J. (1983) *J. Biomol. Struct. Dyn. 1*, 705–714.
Thoma, F., Koller, T., & Klug, A. (1979) *J. Cell Biol. 83*, 403–427.
Thomas, J. O., & Thompson, R. J. (1977) *Cell (Cambridge, Mass.) 10*, 633–640.
Thomas, J. O., & Khabaza, A. J. A. (1980) *Eur. J. Biochem. 112*, 501–511.
Tjerneld, F., Norden, B., & Wallin, H. (1982) *Biopolymers 21*, 343–358.
Woodcock, C. L. F., Frado, L.-L. Y., & Rattner, J. B. (1984) *J. Cell Biol. 99*, 42–52.
Worcel, A., Strogatz, S., & Riley, D. (1981) *Proc. Natl. Acad. Sci. U.S.A. 78*, 1461–1465.
Yabuki, H., Dattagupta, N., & Crothers, D. M. (1982) *Biochemistry 21*, 5015–5020.
Zentgraf, H., Muller, V., & Franke, W. W. (1980a) *Eur. J. Cell Biol. 20*, 254–264.
Zentgraf, H., Muller, V., & Franke, W. W. (1980b) *Eur. J. Cell Biol. 23*, 171–188.

Preferential in Vitro Binding of High Mobility Group Proteins 14 and 17 to Nucleosomes Containing Active and DNase I Sensitive Single-Copy Genes†

Timothy W. Brotherton and Gordon D. Ginder*

Veterans Administration Medical Center and Department of Internal Medicine and Genetics Ph.D. Program, University of Iowa, Iowa City, Iowa 52242

Received October 25, 1985; Revised Manuscript Received January 30, 1986

ABSTRACT: High mobility group (HMG) proteins 14 and 17 bind to mononucleosomes in vitro, but the exact nature of this binding has not been clearly established. A new method was developed to allow direct membrane transfer of DNA from HMG 14/17 bound and unbound nucleosomes, which have been separated by acrylamide gel electrophoresis. Hybridization analysis of membranes obtained by this method revealed that the HMG 14/17 bound nucleosomes of avian erythrocytes and rat hepatic tumor (HTC) cells were enriched, about 2-fold, in actively transcribed genes and also inactive but DNase I sensitive genes. Nucleosomes containing inactive, DNase I resistant genes were bound by HMG 14/17, but not preferentially. Several factors that have been reported to greatly influence the binding of HMG 14/17 to nucleosomes in vitro were tested and shown to not account for the preferential binding to DNase I sensitive chromatin. These factors include nucleosomal linker DNA length, single-stranded DNA nicks, and DNA bulk hypomethylation. An additional factor, histone acetylation, was preferentially associated with the HMG 14/17 bound chromatin fraction of avian erythrocytes, but it was not associated with the HMG 14/17 bound chromatin fraction of metabolically active HTC cells. The latter finding was true for all kinetic forms of histone acetylation.

The organization of chromatin in the eukaryotic nucleus is thought to play an important part in the regulation of gene activity [for review, see Cartwright et al. (1982)]. At the first level of organization, DNA is assembled with histones into structures called nucleosomes. Although both transcriptionally active and inactive DNA are contained in nucleosomes (Cartwright et al., 1982), distinct structural differences must exist between these states since transcriptionally active chromatin has an enhanced sensitivity to the pancreatic-derived nuclease DNase I compared to the bulk of chromatin (Weintraub & Groudine, 1976). While the ultimate features of chromatin that direct this sensitivity are unknown, the high mobility group (HMG)[1] proteins 14 and 17 have been considered as possible mediators of the enhanced digestion of active chromatin by DNase I. This consideration is based on the observation that 0.35 M salt washing of nuclei or nucleosomes, a treatment that removes a number of non-histone proteins, results in a loss of the nuclease sensitivity of active genes and that this sensitivity can be restored by the readdition of purified HMG 14/17 proteins (Weisbrod & Weintraub, 1979; Gazit et al., 1980). Further attempts to associate HMG 14/17 proteins with transcriptionally active chromatin have given conflicting results and, thus, have been inconclusive (Levy et al., 1977; Levy & Dixon, 1978; Goodwin et al., 1979; Albanese & Weintraub, 1980; Sandeen et al., 1980; Barsoum et al., 1981; Levinger et al., 1981; Weisbrod, 1982; Nicolas et al., 1983; Swerdlow & Varshavsky, 1983). The role of HMG 14/17 proteins in mediating DNase I sensitivity has also been recently questioned (Nicolas et al., 1983; Seale et al., 1983; Goodwin et al., 1985).

The HMG 14/17 proteins are present together in nuclei at about one copy each per ten nucleosomes (Mayes, 1982), and both interact with the nucleosome at the junction between core and linker DNA (Goodwin et al., 1979; Sandeen et al., 1980; Mardian et al., 1980). However, the features of nucleosomal preparations that direct HMG 14/17 binding are not known. Various factors that have been implicated in preferential binding in vitro include nucleosomal DNA length (Goodwin

† This was supported by a Basil O'Connor Starter Research Grant from the March of Dimes and NIH Grant AM 29902 to G.D.G., who is a Clinical Investigator of the VA, and by NIH Institutional Grant NRSA HL07344.

* Address correspondence to this author at the Division of Hematology-Oncology, Department of Internal Medicine, University of Iowa College of Medicine, Iowa City, IA 52242.

[1] Abbreviations: HMG, high mobility group proteins; CRBC, chicken red blood cells; HTC, rat hepatic tumor cell line; TAT, tyrosine aminotransferase; SDS, sodium dodecyl sulfate; bp, base pairs; kbp, kilobase pairs; AZA, 5-azacytidine; Tris-HCl, tris(hydroxymethyl)aminomethane hydrochloride; EDTA, ethylenediaminetetraacetic acid.

0006-2960/86/0425-3447$01.50/0